Forest Ecology and Management 530 (2023) 120761

Contents lists available at ScienceDirect

Forest Ecology and Management

journal homepage: www.elsevier.com/locate/foreco

Development of tools to estimate the contribution of young sweet chestnut plantations to climate-change mitigation

M. Menéndez-Miguélez [a,*], P. Álvarez-Álvarez [b], M. Pardos [a], G. Madrigal [a], R. Ruiz-Peinado [a], E. López-Senespleda [a], M. Del Río [a], R. Calama [a]

[a] Instituto de Ciencias Forestales (ICIFOR-INIA), CSIC, Crta. La Coruña, km 7.5, 28040 Madrid, Spain
[b] Department of Organisms and Systems Biology, Polytechnic School of Mieres, University of Oviedo, E-33600 Mieres, Asturias, Spain

ARTICLE INFO

Keywords:
Castanea sativa
Reforestations
Individual tree
Stand
Biomass estimation
LULUCF
Climate change mitigation

ABSTRACT

Sweet chestnut plantations, irrespective of their main productive orientation (nut or timber production), are key elements of the landscape as well as the cultural heritage of the areas where they are found and provide important functions and services. Hence, recent initiatives have been aimed at extending the area occupied by chestnut trees through forest plantations. Nevertheless, the role of these young chestnut plantations as carbon sinks has been often ignored. The National Inventory of Greenhouse Gas Emissions (GHG) must include estimates of the so-called 'transition forests' during the 20 years following their plantation.

In this study, new tools for estimating the total amount of above and belowground biomass stored in young plantations of chestnut were developed to quantify the carbon storage capacity of these plantations. A new set of aboveground biomass and root-shoot ratio models were fitted for individual-tree level based on four different independent variables – root collar diameter, total height, diameter at breast height and crown projection area – and their combinations. The expansion to stand level was based on age, plantation density, productive orientation of the plantation (nut or timber), site index and climate covariates as possible independent variables. At tree level, the best aboveground biomass models were those that include the product of root-collar or breast height diameters and tree height, whereas for root-shoot ratio the best results were obtained when only diameter at breast height is included. At stand level, the most accurate models included age, plantation density and site index for aboveground biomass and only age for root-shoot ratio. The fitted models provided accurate and unbiased predictions of aboveground biomass in the first years of reforestations.

The different fitted equations can be used to estimate carbon stocks in young plantations depending on the available data and the objective of the prediction. Individual tree-level equations are recommended when accurate estimates are needed and detailed inventory measurements are available. Stand level equations, only using plantation age, can be an appropriate alternative for use with forest statistics at national scale, although the inclusion of additional covariates can greatly improve the accuracy of the age-based stand level equations. Our results indicated that even low-density nut-oriented chestnut plantations can play a relevant role as C sinks.

1. Introduction

Trees and forests capture atmospheric C by means of photosynthetic activity, which helps to regulate the climate and reduce the concentration of greenhouse gases. The restoration of forests and increase in forested area through afforestation and reforestation have been reproposed as effective tools to mitigate climate change by slowing CO_2 accumulation in the atmosphere, thus mitigating climate warming (Chazdon and Brancalion, 2019; Griscom et al., 2017; Lee et al., 2018).

International initiatives such as the United Nations Decade (2021–2030) on Ecosystem Restoration, the 1 Trillion Trees Initiative of the World Economic Forum, the Bonn Challenge to restore 350 million ha by 2030, or the plantation of 3 billion trees in the UE by 2030 through the Forest Strategy, highlight the recognition of this important role as a C sink. Despite this rising interest in reforestation as an approach to climate change mitigation, high uncertainty exists around the potential of C capture by new forest land (Lewis et al., 2019). An accurate assessment of the potential for C uptake in new reforestations is

* Corresponding author.
E-mail address: menendez.maria@inia.csic.es (M. Menéndez-Miguélez).

https://doi.org/10.1016/j.foreco.2022.120761
Received 24 October 2022; Received in revised form 16 December 2022; Accepted 23 December 2022
Available online 31 December 2022

required, since these areas must be considered in Land Use, Land Use Change and Forestry (LULUCF) statistics, as well as in national inventories of greenhouse gases (GHG). Until now, C uptake quantification in new reforestations has commonly been carried out using methods developed for adult and natural stands, which may lead to biased and inaccurate estimations of C stocks during the first years after afforestation (Menéndez-Miguélez et al., 2022a). Most of the existing biomass equations for tree species have been developed for trees with diameter at breast height over 7–10 cm, which is the minimum threshold used in forest inventories, and only a few individual tree-level biomass equations for young afforestations have recently been developed for some forest species (Annighöfer et al., 2016; Menéndez-Miguélez et al., 2022a, 2022b).

Regarding the estimation of biomass at stand level, the scaling-up approach is one of the most commonly used methods at local scales. This method consists of using previously developed individual-tree-biomass models to predict stand biomass as the sum of the predicted biomass of individual trees (e.g., Balboa-Murias et al., 2006). When the aim is to estimate biomass in larger management areas with limited forest inventory data, more efficient estimation methods such as stand biomass equations (SBE) or biomass expansion factors (BEF) must be used (Somogyi et al., 2007). Most of the stand-level models developed predict biomass using stand variables such as dominant height and/or stand basal area, although these variables are not frequently available for young afforestations. Moreover, other variables commonly ignored in these equations, such as plantation age, initial plantation density or early site management and soil preparation can be critical parameters for characterizing young plantations (Waring et al., 2020). Thus, precise assessment of the C uptake capacity of reforestations during their initial stages requires the development of specific tools and methods.

Chestnut (*Castanea sativa* Mill.) covers >2.5 million hectares in Europe, distributed from the Southern Mediterranean to Central, Atlantic, and Eastern Europe (Conedera et al., 2004a). In Spain, chestnut is a native species (Conedera et al., 2004b; Krebs et al., 2019; Roces-Díaz et al., 2018a) distributed across an area of 272,400 ha, of which 154,500 ha are pure stands (chestnut cover rate $\geq$ 60 %). The existing chestnut woodland differs widely in terms of the main productive aim (nut or wood production) and stand structure (coppice stands or high forest), implying different stand densities and therefore, different amounts of C fixation. The establishment of new chestnut agroforestry plantations oriented to fruit production is one of the main actions required to promote, conserve and recover traditional landscape in rural areas (Díaz-Varela et al., 2018, Castedo-Dorado et al., 2021). Moreover, the role of timber-oriented plantations, devoted to high-quality timber production (Lemaire, 2008) or even to biomass production under short-rotations (McKay et al., 2022) will be maintained, especially in areas with high rainfall (Pereira-Lorenzo and Ramos Cabrer, 2004). Despite this recognized importance of chestnut as a source of different services and provisions, as well as the recent initiatives to extend the area occupied by the species, the role that could be played by young chestnut plantations in carbon capture (sink effect) and accumulation (reservoir effect), and therefore in mitigating climate change, has been largely ignored (EUROCASTANEA, 2019). This may be due, on the one hand, to the agronomic or agroforestry character of these plantations (especially nut-oriented plantations), commonly occupying former arable land. On the other hand, the fact that these plantations tend to be small and privately owned means that many of them are neither considered in the forest statistics nor integrated in the LULUCF statistics. Furthermore, the lack of reliable, accurate tools for assessing biomass and C fixation in these plantations may hinder the task.

Individual tree biomass, aboveground stand biomass along with their yearly increments and nutrient contents have been studied in chestnut coppices in Spain, Italy and France (Bédéneau, 1988; Cutini, 2000; Santa Regina, 2000; Menéndez-Miguélez et al., 2015) as well as in high forest in both Portugal (Patrício et al., 2005; Patrício, 2006; Patrício and Nunes, 2017; Patrício and Tomé, 2018) and Spain (Ruiz-Peinado et al., 2012). However, all of these studies focus on adult stands, thus their findings are not applicable to biomass estimation or C quantification in the initial stages of reforestation.

The main aim of this study is to provide new tools for determining the total amount of aboveground and belowground biomass stored by young chestnut plantations during the initial stages (<25 years) and to quantify the biomass storage capacity of these plantations. Two modelling approaches were used:

- Individual-tree-level models which use different tree-level attributes as predictors (crown size, height and both root collar and diameter at breast height). Their main use is to estimate total biomass of the plantation using detailed data at tree level from field or remote sensing based inventory.

- A set of models for total biomass stored in the plantation per hectare (stand level), using plantation age and other easy-to-measure plantation characteristics, such as density, productive orientation, site index or mean climate traits as predictors. These models allow us to estimate the biomass stored in young chestnut plantations in those cases where scarce information is available at stand level, as is the case of national or regional forest statistics.

We hypothesized that: (*i*) combining different tree variables results in more accurate predictions of the biomass of each tree; (*ii*) plantation age combined with other plantation characteristics that are simpler to determine may be as efficient in predicting total biomass as the models involving dendrometric covariates measured from field inventories; (*iii*) the capacity of young chestnut plantations as atmospheric C sinks, even in the low density nut-oriented plantations, is similar to the capacity of other forest plantations commonly used in the territory.

2. Material and methods

2.1. Material

2.1.1. Network of plots

Since the main aim of the study was to construct biomass equations with countrywide geographical validity (Spain), we attempted to identify young chestnut plantations throughout the whole area in which the species occurs (Fig. 1). Plantations were selected such that the wide range of environmental conditions identified was embraced (annual rainfall: 700–1600 mm, mean annual temperature: 11–15 °C), with ages ranging between 2 and 28 years. The selected plantations included both plantations with native sweet chestnut (*Castanea sativa* Mill.) or hybrids selected for their high timber-quality or nut productivity. The plantations are representative of the different management alternatives found across the territory. Given the difficulty involved in identifying the exact hybrid used, or the fact that some plantations include different hybrids mixed with *C. sativa* trees, the clone or variety was not considered as a potential predictor, and all plantations were pooled in a single data set. Based on the initial density, plantations were classified as timber-oriented (those over 400 stems ha^{-1} initially) and nut-oriented, those with an initial density below this value (Roces-Díaz et al., 2018b) (see Fig. 2). The dataset included seventy-six plots, of which thirty-two were specifically installed by INIA-CSIC (henceforth INIA plots) in the framework of the current study. These plots cover the whole set of Spanish regions in which the species has recently been used in reforestations. The remaining forty-four plots belong to a network installed in 2010 by the University of Oviedo (henceforth UNIOVI plots) in young chestnut plantations at different locations in NW Spain. Table S.1 in *Supplementary material* includes a detailed list of the sampled plots.

Plots from both data sets have similar characteristics; they are rectangular, with variable size (200 m^2 – 20000 m^2), aiming to include at least 25 trees, and with similar inventory protocols. For all the trees included in the plots, root-collar diameter (*RCD*, cm), diameter at breast height (*dbh*, cm) (once reached) and total height (*h*, m) were measured. From these data, plot level variables were also computed, namely,

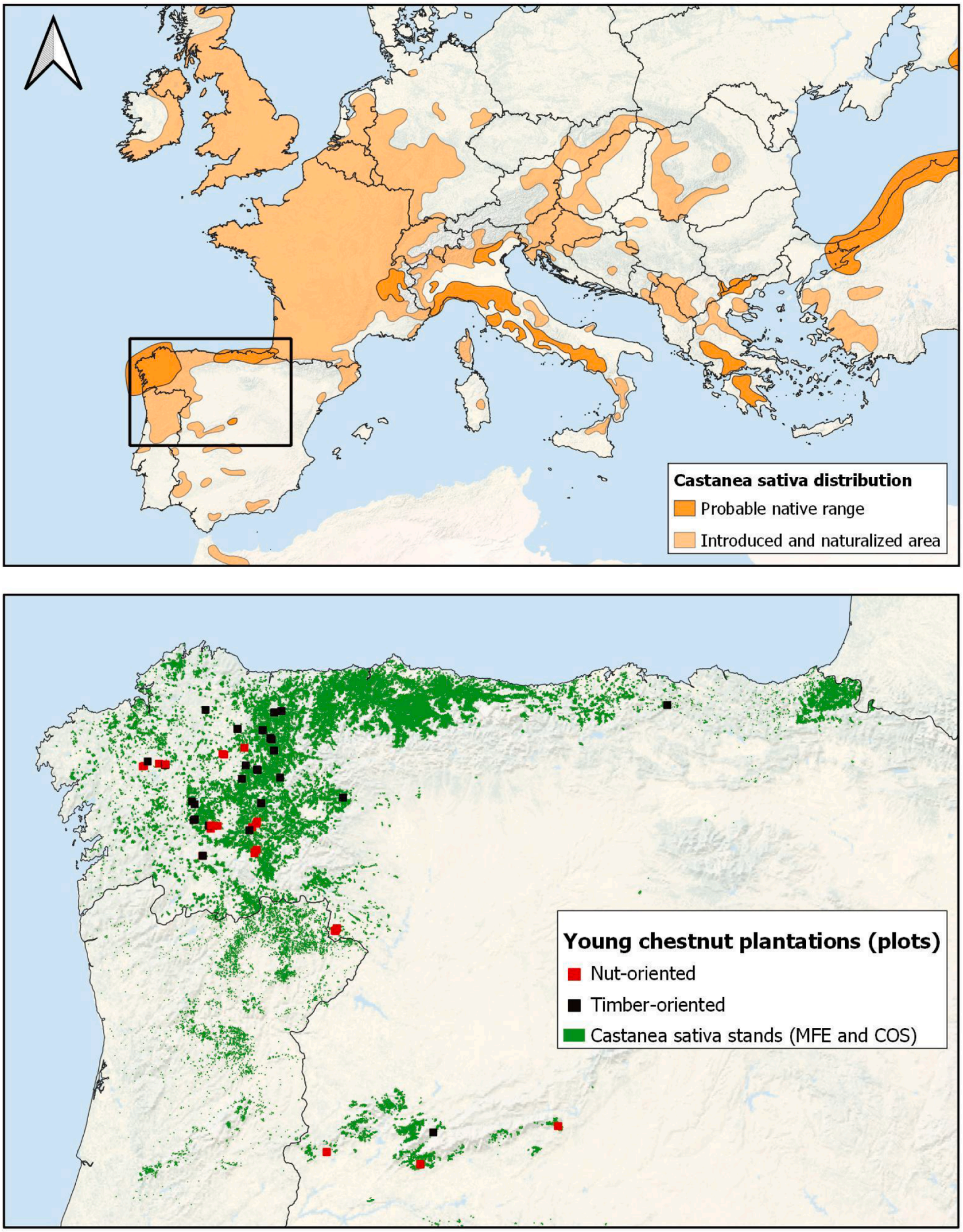

Fig. 1. Plot location. Each square corresponds to 1–5 neighbouring plots.

number of trees per hectare (*N*), mean height (*Hm*, m), mean diameter (*dm*) and Weise dominant height (*H*o), defined as the mean height of the 20 % thickest trees per hectare (Table 1). For UNIOVI plots, only the mean plot level values were available. Additional information for slope, aspect, soil preparation technique, percentage of failures in the reforestation, accompanying vegetation, etc. was also collected during the inventory. Plantation age was assessed after consulting with owners and Forest Services, and in case of doubt, confirmed using historical aerial photographs. Mean climatic values (mean annual rainfall and mean annual temperature) were derived for each plot from the climatic model by Gonzalo et al. (2010). Plot dominant height and plantation age were used to compute site index (*SI*), defined as the dominant height (m) of the plot at a plantation age of 10 years, using the site index model by Álvarez-Álvarez et al. (2010), specifically constructed for young chestnut plantations:

$$SI = H_o \cdot \left[\frac{1 - exp^{(-0.139 \bullet 10)}}{1 - exp^{(-0.139 \bullet T)}}\right]^{0.886} \quad [1]$$

where H_0 represents plot dominant height at age T.

Fig. 2. Timber-oriented chestnut plantation (above, density 693 stems ha^{-1}, age 10 years) and nut-oriented plantation (below, density 125 stems ha^{-1}, age 14 years).

Table 1
Descriptive statistics for the main attributes recorded at plot level.

	Nut oriented ($n = 41$)			Timber-oriented ($n = 35$)		
Attribute	**Mean**	**Min**	**Max**	**Mean**	**Min**	**Max**
N (trees ha^{-1})	199	59	394	715	400	1942
Age (years)	11.1	2.0	28.0	9.0	2.0	20.0
H_m (m)	5.32	1.20	9.57	5.34	0.88	11.65
H_0 (m)	6.66	1.65	11.25	6.87	1.43	14.10
d_m (cm)	11.18	0.21	36.21	7.19	0.06	25.40
SI (m)	6.7	2.6	9.7	7.5	3.9	11.7
Rainfall (mm)	1034	706	1587	1257	857	1557
Tm (°C)	12.6	12.6	15.0	11.3	11.3	13.6

Note. *N* is the stand density, H_m is the average height, H_0 is the dominant height, *dm* is the mean diameter, SI is the site index, Tm is the mean annual temperature.

2.1.2. Sampled trees

To estimate tree-level biomass, 31 trees with average growing conditions were destructively sampled in a subsample of 10 INIA plots, covering an age range of 4 – 28 years. In each of these plots three trees were selected, belonging to the lowest, middle and highest tercile of the height distribution. In addition to the tree-level measurements carried out during plot inventory, two perpendicular crown diameters (*dc*, cm) were also measured for each sample tree before felling. The two perpendicular crown diameters allowed the crown projection area (*CPA*, m^2) to be estimated along with biomass-packing (*BP*, m^3), defined as the product between tree height and crown projection area (*CPA*). Sampled trees were felled, separated into biomass components and weighed in the field to obtain the fresh weight of each component. A procedure similar to that proposed by Montero et al. (1999, 2005) was adapted to the small size of the plants, dividing them into only two compartments, (i) stem and branches with diameter over > 2 cm, and (ii) branches with diameter less than < 2 cm and leaves. In addition, in a subset of 12 trees (aiming to cover all the range of observed root collar diameters), root system was extracted using a backhoe digger, and weighed in the field. Difficulties for the digging machinery to enter the plantations prevented us from sampling more roots.

Representative composite samples were taken to the laboratory and oven-dried at 102 °C to determine humidity. Humidity of these samples was then applied to the fresh measured-at-field weight to determine the dry weight of each component. For this study, stems, branches and leaves were finally grouped as aboveground biomass (AGB), while roots (when available) defined the belowground biomass. For further information on the field and laboratory procedures, see Menéndez-Miguélez et al. (2022a). Mean data on the destructive sampling is shown on Table 2.

2.2. Methods

2.2.1. Biomass and root-shoot equations at tree level

The most common mathematical model used for biomass prediction takes the form of Snell (1892) power function $y = \beta_0 \bullet x^{\beta_1}$ (Kaitaniemi, 2004; Zianis et al., 2005; Zianis and Mencuccini, 2004). For model fitting purposes, we preferred to use nonlinear models in order to maintain the additive structure of the residuals and avoid the inherent bias associated with logarithmic-transformed linear models. This nonlinear model was tested to relate aboveground tree biomass with tree variables measured in the field such as RD, *dbh*, total height or crown projection area (models 2.1–2.4). Three additional models with a combination of tree variables were also tested, using RCD^2h (model 2.5), d^2h (model 2.6) and the *BP* (model 2.7) as independent covariates:

$$AGB = \beta_0 \bullet RCD^{\beta_1} \quad [2.1]$$

$$AGB = \beta_0 \bullet h^{\beta_1} \quad [2.2]$$

$$AGB = \beta_0 \bullet CPA^{\beta_1} \quad [2.3]$$

$$AGB = \beta_0 \bullet (dbh)^{\beta_1} \quad [2.4]$$

$$AGB = \beta_0 \bullet \left(RCD^2h\right)^{\beta_1} \quad [2.5]$$

$$AGB = \beta_0 \bullet \left(dbh^2h\right)^{\beta_1} \quad [2.6]$$

$$AGB = \beta_0 \bullet BP^{\beta_1} \quad [2.7]$$

where *AGB* is the aboveground dry biomass (kg), *RCD* is the root-collar-diameter (cm), *dbh* is diameter at breast height (cm), *h* is the total tree height (m), *CPA* is the crown projection area (m^2), *BP* is the biomass packing (crown projection area * height, m^3), β_i are the parameters of the model.

For belowground biomass, we computed the root-shoot ratio (dry weight of the roots divided by the dry weight of the stem and branch fractions) and aimed to relate this attribute with the same explanatory covariates using the power function (referred to in the Results section as

Table 2
Mean attributes of the trees destructively sampled for biomass estimation.

Attribute	*n*	*mean*	*min*	*max*
RCD (cm)	31	16.04	5.40	34.00
dbh (cm)	31	13.56	1.30	33.60
h (m)	31	6.14	2.78	9.70
CPA (m^2)	31	11.55	0.44	45.96
AGB (kg dry matter $tree^{-1}$)	31	57.53	1.35	179.06
BGB (kg dry matter $tree^{-1}$)	12	17.41	2.90	49.30
Root-shoot ratio	12	0.594	0.187	1.716

Note. *RCD* is the root collar diameter, *dbh* is the diameter at breast height, *h* is the total height, *CPA* is the crown projection area, *AGB* is the total aboveground biomass, *BGB* is the belowground biomass.

models [2.8] to [2.14]). Given the small size of the sample, and the well-known allometric relationship between above and belowground biomass (Kurz et al., 1996) we preferred to use root-shoot ratio instead of directly modelling root weight. The advantage of this ratio is that it can be applied to individual trees or stands, at local, regional or landscape level (Mokany et al., 2006), and is commonly used in National Greenhouse Gas Inventories.

2.2.2. Aboveground biomass equations at stand level

The best equation identified in the previous section was then used to compute aboveground biomass for every tree within each INIA plot (b_{tree}). The sum of the individual values of tree biomass gives the aboveground biomass for the plot, which was then upscaled to the hectare to obtain total aboveground biomass per ha (W_{ha}, kg dry matter. ha^{-1}). In the case of the UNIOVI plots, since no data were available at individual tree level, we used data from INIA plots to construct an auxiliary model for predicting the mean value of aboveground tree biomass within the plot. This value was then upscaled to the hectare by multiplying it by the plantation density (N, stems ha^{-1}) to calculate total aboveground biomass per ha (W_{ha}, kg dry matter. ha^{-1}). See supplementary material S3 for additional information on this model for mean tree biomass.

The aim of the study was to construct models to predict total aboveground biomass W_{ha} in young chestnut plantations using plantation age as well as other easily obtained covariates (not involving complex field-based forest measurements). To do this, first we proposed to fit a simple model which only depends on plantation age T (years):

$$W_{ha} = aT^{b} \quad [4]$$

In a second phase, we evaluated the expansion of parameters a and b by including a single additional explanatory covariate X_1:

$$W_{ha} = (a_0 + a_1X_1)T^{(b_0+b_1X_1)} \quad [5]$$

As potential explanatory covariate X_1 we tested:

- Plantation density N (stems ha^{-1}).
- Plantation productive orientation, by creating a dummy variable *Nut*, with a value 1 if the plantation is nut oriented (i.e. stand density below 400 stems ha^{-1}) and zero if it is timber oriented.
- Site index *SI* for the plantation (m), computed according to Álvarez-Álvarez et al. (2010), and specifically built for young chestnut plantations.
- Climate covariates: annual cumulative rainfall (mm) and mean annual temperature (°C) calculated for the plantation from the climatic models by Gonzalo et al. (2010).

For each individual covariate we compared the complete model [5] (including the additional explanatory covariate in both parameters a and b) with reduced models, considering the expansion of only one of the parameters and with the general basic model in eq. [4]. Comparisons among nested models were made by means of the *Non-linear extra sum-of-squares F-test* (Calama et al., 2003; Huang et al., 2000; Pillsbury et al., 1995). This F-test uses the following statistic:

$$F = \frac{\left[\frac{SS_r - SS_f}{df_r - df_f}\right]}{\left[\frac{SS_f}{df_f}\right]} \quad [6]$$

where SS_f and SS_r refers to the sum of the squared error for the complete and the reduced model, and df_f and df_r the degrees of freedom for complete and reduced model, respectively. If F statistics is distributed as a $F_{\textit{Fisher-Snedecor}}$ with parameters (1–α; df_r–df_f; df_f) we cannot reject the null hypothesis of the reduced model explaining as much variability as the complete one, and we will therefore select the reduced model. As an additional criterion, the level of significance of the parameters was checked.

Once we had selected the best model for age and each single additional covariate, we explored the inclusion of a potential second covariate X_2.

$$W_{ha} = (a_0 + a_1X_1 + a_2X_2)T^{(b_0+b_1X_1+b_2X_2)} \quad [7]$$

For the sake of simplicity and to prevent multicollinearity we imposed the following constraints:

- A model cannot simultaneously include the two stocking related covariables (N or *Nut*) as predictors.
- Only the best climate covariate (annual rainfall or annual mean temperature) identified in the fitting of the one-single-predictor models would be evaluated in this second phase.
- A model cannot simultaneously include the two environmental related variables (*Site index* or the *best climate covariate*) as predictors.

As in the previous phase, we evaluated the different possible alternatives for entering the covariates X_1 and X_2 in the parameter a and b of the model by comparing the complete model [7] with different reduced models through the Non-linear extra sum-of-squares *F-test.*

Root-shoot ratio models for individual-tree level were used to compute the root-shoot ratio for each tree within the plots, and therefore to compute the mean value of the ratio for the plot. Given the available data, only that from the network of INIA plots was used to fit this model. This mean root-shoot ratio was modelled as a function of plantation age using the power function. Given the small size of the sample and the high uncertainty associated, we did not consider the inclusion of other potential covariates apart from age.

For all the fitted models we first carried out a preliminary fitting using ordinary non-linear least squares techniques and residuals were checked for heteroscedasticity, a common problem associated with biomass models. If detected, we fitted the models using Weighted non-linear least squares, where each observation was corrected by weighting it with the inverse of its residual variance. As an independent sample was not available for validation, we carried out a leave-out-one cross validation (LOOCV, Sammut and Webb, 2011) of the selected models. In this method we refitted each model k times (where k is the sample size), assuming that at each replicate one of the observations is removed, and then applied the so-fitted model to this observation and compute the LOOCV residuals. All the models were fitted using the SAS/STAT® NLIN and SAS/ETS® MODEL procedures (SAS Inc., 2004). The behaviour of the different fitted models was evaluated by means of the root of mean squared error (RMSE) and R^2_{adj}. Although all the fitted models allow biomass to be estimated in terms of dry matter, C storage capacity can easily be assessed using the tabulated value of C content for the species as reported in Montero et al. (2005).

3. Results

3.1. Biomass and root-shoot equations at individual tree level

Table 3 shows the parameter estimates and goodness-of-fit statistics

Table 3
Parameter estimates and goodness-of-fit statistics for the models of individual tree aboveground biomass.

Model	Covariate	β_0	β_1	RMSE	R^2_{adj}
[2.1]	*RCD*	0.6258	1.0641	22.4897	0.8382
[2.2]	*h*	0.7059	2.3604	50.2156	0.1938
[2.3]	*CPA*	4.2332	0.9851	31.7554	0.6776
[2.4]	*dbh*	0.8238	1.5324	22.8726	0.8327
[2.5]	RCD^2h	0.0919	0.8419	18.1903	0.8942
[2.6]	dbh^2h	0.2074	0.7511	19.1853	0.8823
[2.7]	*BP*	1.1069	0.8922	29.9842	0.7125

Note. β_j are fitting parameters, RMSE is the root mean square error, R^2_{adj} is the adjusted coefficient of determination.

for the biomass models at tree level using different tree-size attributes. All the models and parameter estimates were highly significant, and reached values of R^2_{adj} over 0.65, except for the model which only included tree height as a predictor. The best results were obtained for models 2.1 and 2.5, which used the product between the square *RCD* or the squared *dbh* in combination with total tree height as predictors, reaching R^2_{adj} close to 0.90. The models which only included *d* or *RCD* reached values over 0.83, while the models which included crown-size related attributes (*CPA* and *BP*) explained over 0.67 – 0.70 of the observed variability. In contrast, we observed that height was not a good predictor – when used alone – of individual tree biomass. Cross-validation statistics (Table S.5) reveal a similar behaviour, reinforcing the robustness of the models.

Individual-tree-level models for root-shoot ratio (Table 4) revealed a similar behaviour to that of the models for aboveground biomass of trees, with the only exception being that the best predictor was *dbh* (R^2_{adj} = 0.6686, parameter β_0 = 1.8887, parameter β_1 = -0.6296).

3.2. Aboveground biomass and root-shoot ratio equations at stand level

The basic stand-level biomass model (eq. [4]), where only plantation age was used as a predictor, resulted in low predictive accuracy (R^2_{adj} = 0.2029, RMSE > 18000 kg ha^{-1}) (Table 5), with high uncertainty in the estimates for older plots (Fig. 3).

In the next step we expanded the original parameters of the power function in eq.4 to test the inclusion of a single additional covariate (see Table S.2 in *Supplementary material*). The results for parameter estimates and goodness-of-fit statistics of the selected model for each covariate are shown in Table 5. The results of the sequential procedure indicated that, in this first step, the individual covariate that best explained observed variability was plantation density (*N*), entered in parameter *a*, reaching a R^2_{adj} close to 0.80. Expansion of parameter *b* over site index or productive orientation (dummy covariate *Nut*) resulted in R^2_{adj} values over 0.71, while expansion of both parameters *a* and *b* over annual rainfall reached R^2_{adj} of 0.69. In contrast, the inclusion of mean annual temperature in the model did not lead to a significant improvement (*p-value* 0.1283) with respect to the basic model [4], so this covariate was not tested in further analyses. The results showed that, as expected, existing biomass per hectare increases as plantation density, annual rainfall or site index increases. Furthermore, timber oriented plantations are much more productive in terms of biomass growth than nut oriented ones (Fig. 4).

Table S.3 in the *Supplementary material* shows the sequential procedure for the biomass models including two covariates, according to the proposed expansion in model [7], while parameter estimates and goodness-of-fit statistics of the best model for each combination of covariates are shown in Table 5. Table S.3 shows that the inclusion of a second covariate leads to a significant improvement over the single-covariate models. The best selected model was that which included *SI* in both parameters *a* and *b*, and plantation density only in parameter b, resulting in the five-parameter model 9.2 (see table 5), which reached a R^2_{adj} over 0.9314 and RMSE of 5350 kg ha^{-1}. Models including the *Nut* productive orientation and site index (model 7.7) along with density and annual rainfall (model 10.9) reached similar R^2_{adj} values of around 0.86. Finally, model 8.9, expanding parameter *b* over both *Nut* and *Rainfall,* reached a R^2_{adj} value of 0.75. Similar values were identified in the cross-validation process (Table S.6 in *Supplementary material*), confirming the validity of the models.

Finally, the fitted model for the mean root-shoot ratio (Table 6, Fig. 5) showed a clear decreasing pattern, with a trend towards stabilisation at plantation ages over 15–20 years (Table 6, Fig. 5).

Table 4
Parameter estimates and goodness-of-fit statistics for the models for individual root-shoot ratio.

Model	Covariate	β_0	β_1	RMSE	R^2_{adj}
[2.8]	*RCD*	13.2183	−1.3458	0.2457	0.6370
[2.9]	*h*	6.5297	−1.5962	0.2824	0.5202
[2.10]	*CPA*	0.8410	−0.4790	0.2854	0.5102
[2.11]	*dbh*	1.8887	−0.6296	0.2347	0.6686
[2.12]	RCD^2h	13.8963	−0.5199	0.2532	0.6146
[2.13]	dbh^2h	2.3718	−0.2676	0.2386	0.6577
[2.14]	*BP*	1.4472	−0.3959	0.2798	0.5292

Note. β_j are fitting parameters, RMSE is the root mean square error, R^2_{adj} is the adjusted coefficient of determination.

4. Discussion

In this study, we develop different sets of equations for predicting above and belowground biomass at both tree and stand (plot) levels for young chestnut plantations. Regarding individual-tree biomass equations, previously existing models for the species were mainly developed using data from coppice forests or from high mature forests (Cutini, 2000; Menéndez-Miguélez et al., 2013; Patrício et al., 2005; Ruiz-Peinado et al., 2012; Salazar et al., 2010). These models have a limited capacity for use in young reforestations, since they were fitted using trees with *dbh* > 10 cm, further compounded by the fact that biomass allocation within the tree shifts with tree ontogeny and developmental stage (Xiang et al., 2021).

The set of individual-tree fitted equations valid for young plantations (age < 25 years) used *RCD*, *dbh*, *h*, *CPA* and different combinations of the previous covariates as predictors. Our results indicate that the highest accuracy at individual-tree level was attained when using the product RCD^2h (R^2_{adj} over 0.89), and the product dbh^2h (R^2_{adj} over 0.88), which is in agreement with findings of previous studies using the few existing biomass equations for young trees (Annighöfer et al., 2016; Menéndez-Miguélez et al., 2022a), although these studies did not include *Castanea* sp. among the studied species. In addition, these results allowed the confirmation of the first hypothesis set out in the study. The use of *RCD* or *dbh* as a single predictor, a much less time-consuming option, results in R^2_{adj} values over 0.83, with a very slight advantage of *RCD* over *dbh*. Given the similar behaviour of *RCD* and *dbh* when used alone or in combination with total height, and taking into account that *RCD* measurement is a challenging task (Menéndez-Miguélez et al., 2022a) due to the presence of branches at the base of the stem, root collar deformities, plant shelters or the need to adopt a crouched position, we recommend using *dbh*, except where plants have not reached a height of 1.30 m. This recommendation is supported by the greater observed correlation between *dbh* and root-shoot ratio for calculating belowground biomass (Ledo et al., 2018). In contrast, the use of total plant height as a single predictor for individual biomass in chestnut led to the poorest results (R^2_{adj} < 0.20), which is consistent with the results obtained by Annighöfer et al. (2016), who found height the worst predictor variable for all species. Finally, crown projection area, either as a single predictor or in combination with height, resulted in less accurate models (R^2_{adj} = 0.68–0.71) than those only considering *dbh* or *RCD*. Since crown-size measurement in field inventories is a time consuming task, the use of these crown-based models is only justified if both crown diameter and/or tree total height are estimated from aerial photographs or airborne laser scanning (e.g. Mäkinen et al., 2006). This set of individual tree-level equations is recommended if detailed inventory measurements (including tree *dbh*, tree *h* and stand density) are available at plot level.

Previously existing stand-level biomass models for the species (Castaño-Santamaría et al., 2013; Menéndez-Miguélez et al., 2013; Prada et al., 2019) present the same limitations as those described above (constructed using adult coppice forests), and use stand density, basal area and mean or dominant height as predictors. In our case, we propose a new set of equations, which are valid for young reforestations, using plantation age as the main predictor (Yamaura et al., 2021). Unlike natural high forests or coppices, stand age is a commonly known trait in young chestnut plantations. Moreover, when using national or regional statistics, plantation age and area are often the only variables available

Table 5
Parameter estimates and goodness-of-fit statistics for basic model [4] and the best selected model for each combination including one (model [5]) or two (model [7]) additional covariates.

Model	X_1	X_2	a_0	a_1	a_2	b_0	b_1	b_2	RMSE	R^2_{adj}
4	–	–	269.7			1.6640			18,621	0.2029
5.3	Nut	–	112.5			2.2686	−0.5721		11,087	0.7135
5.5	Density	–	3.2767	0.1519		2.2198			9363	0.7957
5.9	IS	–	1324.6			0.0520	0.1231		11,077	0.7140
5.10	Rainfall	–	29.6196	−0.0173		0.6935	0.00202		11,354	0.6954
7.7	Nut	IS	−691.5		180.7	1.4673	−0.3538		7765	0.8575
8.9	Nut	Rainfall	41.7066			1.8891	−0.3681	0.00060	10,238	0.7523
9.2	Density	IS	1787.4		−147.6	−1.1235	0.00032	0.2863	5350	0.9314
10.9	Density	Rainfall	9.5388			1.7251	0.00037	0.00091	7781	0.8569

Note. a_j and b_j are fitting parameters, RMSE is the root mean square error, R^2_{adj} is the adjusted coefficient of determination. Model number refers to the codes shown in tables S.2 and S.3 in supplementary material.

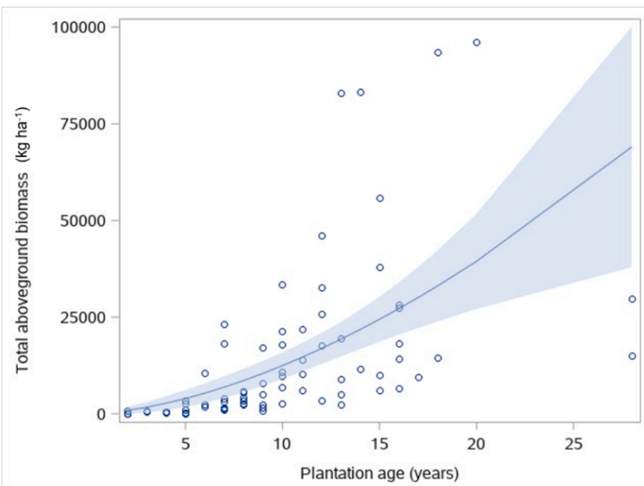

Fig. 3. Observed (dots), fitted line and 95% confidence bands of model 4 for total aboveground biomass as a function of the age of the plantation.

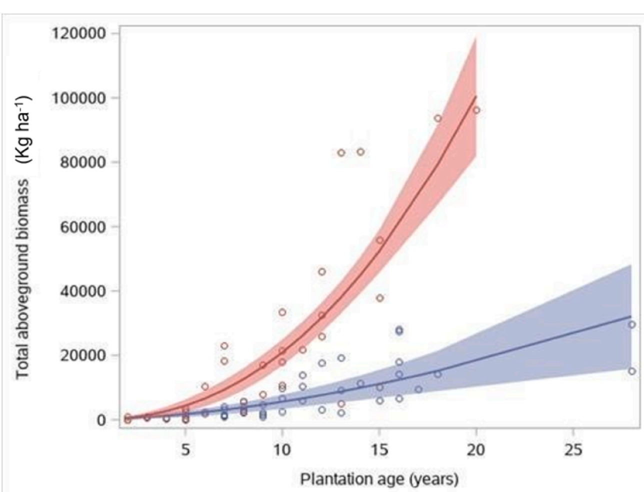

Fig. 4. Observed (dots), fitted line and 95% confidence bands of model 5.3 for total aboveground biomass as a function of the age of the plantation and the productive orientation (nut-oriented in blue, timber-oriented in red). (For interpretation of the references to colour in this figure legend, the reader is referred to the web version of this article.)

to Forest Services, which use these data to estimate the annual carbon fixation capacity by new plantations (e.g. for LULUCF accounts). Our simpler model only includes age as a predictor for both aboveground

Table 6
Parameter estimates and goodness-of-fit statistics for the model for mean root-shoot ratio as a function of plantation age (years).

Response variable	a_0	b_0	RMSE	R^2_{adj}
Root-shoot ratio	3.1052	−0.7437	0.1364	0.6732

Note. a_j and b_j are fitting parameters, RMSE is the root mean square error, R^2_{adj} is the adjusted coefficient of determination.

biomass and root-shoot ratio, without the need for any additional measurements, although the resulting accuracy of the model is low. The more complex models include additional covariates besides plantation age, although the additional measurements proposed are not difficult to measure in the field (tree counting for density and dominant height estimation for site index). Furthermore, the productive orientation (nut-timber) can be considered as a proxy for stand density and can be easily determined by visual observation or query to the owners. Finally, mean annual rainfall may provide a proxy for site index and is easily determined from the geographical coordinates of the plantation.

The inclusion of both site index and plantation density resulted in the most accurate estimates of stand-level biomass ($R^2_{adj} = 0.93$), even comparable to the previously existing models for chestnut coppices using basal area, plantation density and dominant height, thus confirming our second initial hypothesis. The simulations using this model (Fig. 6) reveal that though both site index and stand density have a large influence on aboveground biomass per hectare, changes in site index result in larger productivity increments than those observed in the case of changes in stand density, this finding having previously been reported for chestnut (Castaño-Santamaría et al., 2013). In this regard, it must be noted that the proposed site index model presents high correlation with both soil and climate attributes (see Álvarez-Álvarez et al., 2010), thus accurately capturing the variability observed in these environmental traits.

In addition, plantation density is a reliable indicator of the different management types observed in the area, with lower densities aiming to nut production and higher densities focusing on timber. Either substituting plantation density for productive orientation (*Nut* dummy covariate) or site index for mean annual rainfall in the model resulted in similar predictive accuracy ($R^2_{adj} = 0.86$). Productive orientation, as a categorical *dummy* classification introduced by Roces-Díaz et al. (2018b) using a threshold of 400 stems ha^{-1}, is an accurate predictor, even if entered alone in the model (Fig. 5). As expected, denser timber-oriented plantations display much more efficient C uptake, but the differences in stand density within a given orientation can be compensated by differences in individual tree size. Furthermore, mean annual rainfall is a covariate which is highly correlated with both standing biomass and reforestation success, and was identified as one of the environmental covariates most closely related with site classification in chestnut plantations (Álvarez-Álvarez et al., 2010). Finally, the model which includes both productive orientation and mean annual rainfall has the

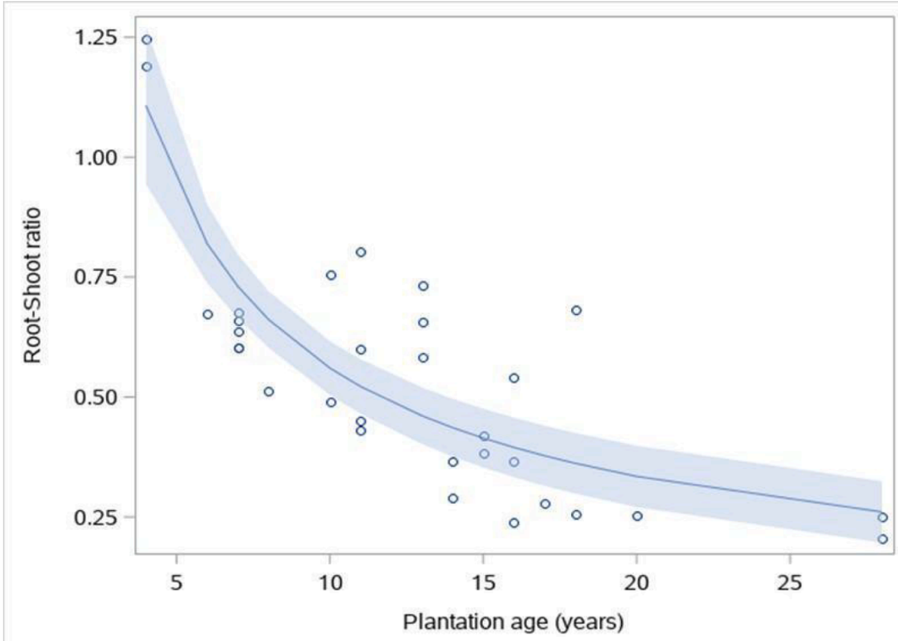

Fig. 5. Observed (dots), fitted line and 95% confidence bands of the model for mean root-shoot ratio as a function of plantation age.

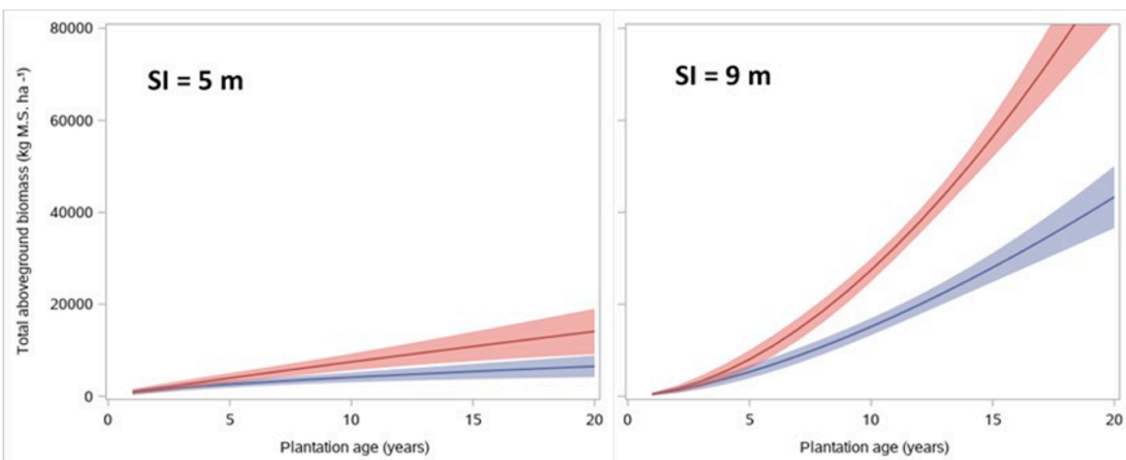

Fig. 6. Total aboveground biomass estimates for a typical timber-oriented (red, 1000 stems.ha^{-1}) and nut-oriented (blue, 200 stems.ha^{-1}) chestnut plantation with site index = 5 m or site index = 9 m, at a reference age of 10 years. (For interpretation of the references to colour in this figure legend, the reader is referred to the web version of this article.)

lowest accuracy. However, since it does not require additional measurements and can be spatially upscaled to regional level, it may provide a useful tool for classifying the territory according to the potential for C fixation.

Both our observations and simulations indicate that a mean, timber-oriented, 20 year-old chestnut plantation may have a total aboveground biomass of 100 Mg ha^{-1}, while at the same age a mean, nut-oriented plantation will reach 20 Mg ha^{-1}, with an expected root-shoot ratio of 25 %. Values for new timber-oriented plantations are of the same order as those proposed for chestnut coppices in Spain by Menéndez-Miguélez et al. (2016), who found values close to 100 Mg ha^{-1} across a wide range of ecological and management conditions in a 20 year-old coppice stand. Nevertheless, our values are below those given for young chestnut plantations in N America (180 Mg ha^{-1} at 19 years, Jacobs et al. (2009)) or coppices in Great Britain (200 Mg ha^{-1} at 20 years, Brasika et al. (2017)). The biomass growth capacity for timber-oriented chestnut plantations located in humid areas of NW Spain (>5 Mg ha^{-1}yr^{-1}) is lower than that observed for highly productive *Pinus radiata* or *Eucalyptus* plantations (Pérez-Cruzado et al., 2011), but may be similar to that observed in other productive conifer plantations of *Pinus pinaster* subsp Atl. (Porté et al., 2002) or *Pinus nigra* (unpublished data). On the other hand, nut-oriented plantations in drier areas of inland Spain can reach an average annual growth capacity over 1 Mg ha^{-1}yr^{-1}, a value which is comparable or even larger than those observed in plantations of typical Mediterranean species such as *Quercus ilex, Ceratonia siliqua* or *Pinus pinea* (Lara-Gómez et al., 2020; Palacios-Rodríguez et al., 2022; Menéndez-Miguélez et al., 2022b). Considering both above and belowground biomass, and assuming a carbon content for the species of 48.4 % (Montero et al., 2005), annual C uptake capacity of these plantations during their first 20 years may vary between 2.2 and 11.1 Mg CO_2 eq ha^{-1}yr^{-1} revealing the important contribution of *Castanea* plantations to removing carbon from the atmosphere and storing it and confirming the last hypothesis set out in our study.

Although the models have been fitted using data from Spain, they could easily be adapted to other European regions in which the species is planted, such as France, Italy or Portugal, as long as the ecological conditions and management practices in these regions are similar to those found in Spain (Fernández-López and Alía, 2003; Beccaro et al., 2020). Despite the relevance of these new equations, our approach presented a main potential limitation, related to the restricted sample size (especially in the number of felled trees) compared with the wide range of management practices and ecological conditions observed in the territory. Future research effort should focus on sampling new areas and management conditions in order to construct more robust equations, with a larger range of validity.

5. Conclusions

We present a set of new equations for predicting standing biomass and C stocks retained by trees and stands in young chestnut plantations in Spain. The choice among the proposed equations will depend on the available data and the objective of the prediction. Individual tree-level equations are recommended if detailed inventory measurements are available and accurate estimates at small-farm level are required. Stand-level equations only using plantation age could be applied in forest statistics at national scale. The accuracy of the age-based stand-level equations can be markedly improved if additional covariates are available, including those which are very straightforward to determine such as productive orientation or mean annual rainfall (from climate grid models).

As expected our results reveal the high C uptake capacity of timber-oriented young chestnut plantations. In addition, we demonstrate that despite having traditionally been considered as agroforestry or even agronomic systems, low-density nut-oriented plantations can play an important role as C sinks, which must be taken into account in general statistics of C uptake by forest plantations (e.g. LULUCF accounts). Nevertheless, C uptake should be considered an additional service provided by these plantations, which also play an important role as part of the landscape and cultural heritage of the areas in which the species grows. The new set of equations will allow forest owners and managers to assess the C uptake capacity of the plantations and to consider this an additional and valuable ecosystem service provided by their chestnut farms.

CRediT authorship contribution statement

M. Menéndez-Miguélez: Methodology, Formal analysis, Conceptualization, Writing - original draft. **M. Pardos:** Writing - review & editing. **R. Ruiz-Peinado:** Methodology, Writing - review & editing. **E. López-Senespleda:** Writing - review & editing. **P. Álvarez-Álvarez:** Writing - review & editing. **M. Madrigal:** Writing - review & editing.**M. Del Río:** Writing - review & editing. **R. Calama:** Conceptualization, Funding acquisition, Methodology, Writing - original draft.

Declaration of Competing Interest

The authors declare that they have no known competing financial interests or personal relationships that could have appeared to influence the work reported in this paper.

Data availability

Data will be made available on request.

Acknowledgements

The authors wish to thank CICYTEX (Elena Nieto and Paula Serrano) and CESEFOR Foundation (Roberto Rubio and Darío Arias) for their valuable help in identifying and locating chestnut plantations and contacting farm owners. This research was funded by the Ministry of Science, Innovation and Universities grant number AGL2017-83828-C2-1-R; Ministry of Agriculture, grant number EG17-042-C02-02; and INIA grant number IMP- 2018-004-C02-02. The publication is also part of the CARE4C Project, which has received funding from the European Union's HORIZON 2020 Research and Innovation Program under the Marie Sklodowska-Curie grant agreement N° 778322. We thank Adam Collins for revising and editing the English grammar.

Appendix A. Supplementary data

Supplementary data to this article can be found online at https://doi.org/10.1016/j.foreco.2022.120761.

References

Álvarez-Álvarez, P., Díaz-Varela, E., Cámara-Obregón, A., Afif-Khouri, E., 2010. Relating growth and nutrition to site factors in young chestnut plantations established on agricultural and forest land in northern Spain. Agrofor. Syst. 79, 291–301. https://doi.org/10.1007/s10457-010-9313-z.

Annighöfer, P., Ameztegui, A., Ammer, C., Balandier, P., Bartsch, N., Bolte, A., Coll, L., Collet, C., Ewald, J., Frischbier, N., Gebereyesus, T., Haase, J., Hamm, T., Hirschfelder, B., Huth, F., Kändler, G., Kahl, A., Kawaletz, H., Kuehne, C., Lacointe, A., Lin, N., Löf, M., Malagoli, P., Marquier, A., Müller, S., Promberger, S., Provendier, D., Röhle, H., Sathornkich, J., Schall, P., Scherer-Lorenzen, M., Schröder, J., Seele, C., Weidig, J., Wirth, C., Wolf, H., Wollmerstädt, J., Mund, M., 2016. Species-specific and generic biomass equations for seedlings and saplings of European tree species. Eur. J. For. Res. 135, 313–329.

Balboa-Murias, M., Rodríguez-Soalleiro, R., Merino, A., Álvarez-González, J.G., 2006. Temporal variations and distribution of carbon stocks in aboveground biomass of radiata pine and maritime pine pure stands under different silvicultural alternatives. For. Ecol. Manage. 237, 29–38.

Beccaro, G., Alma, A., Bounous, G., Gomes-Laranjo, J, 2020. The chestnut handbook. Crop and Forest Management. Boca Raton : CRC Press.

Bédéneau, M., 1988. Croissance du taillis de châtaignier en France, premiers résultats. Ann. Sci. For. 45 (3), 265–274.

Brasika, I.B.M., Mason, J., Castellanos, L.B., Samuelsson, M., 2017. The Carbon Sequestration Potential of Converting Sweet Chestnut Coppice Biomass into Biochar, in: 8th International Conference on Agricultural, Biological, Environmental and Medical Sciences (ABEMS-2017). pp. 46–52. https://doi.org/10.17758/eirai.iae1017309.

Calama, R., Cañadas, N., Montero, G., 2003. Inter-regional variability in site index models for even-aged stands of Stone pine (*Pinus pinea* L.) in Spain. Ann. For. Sci. 60, 259–269. https://doi.org/10.1051/forest:2003017.

Castaño-Santamaría, J., Barrio-Anta, M., Álvarez-Álvarez, P., 2013. Regional-scale stand density management diagrams for pyrenean oak (*Quercus pyrenaica* willd.) stands in north-west Spain. IForest 6, 141–149. https://doi.org/10.3832/ifor0880-006.

Castedo-Dorado, F., Álvarez-Álvarez, P., Cuenca Valera, B., Lombardero, M.J., 2021. Local-scale dispersal patterns and susceptibility to *Dryocosmus kuriphilus* in different *Castanea* species and hybrid clones: insights from a field trial. New For. https://doi.org/10.1007/s11056-021-09893-8.

Chazdon, R., Brancalion, P., 2019. Restoring forests as a means to many ends. Science 364, 24–25. https://doi.org/10.1126/science.aax9539.

Conedera, M., Manetti, M.C., Giudici, F., Amorini, E., 2004a. Distribution and economic potential of the Sweet chestnut (*Castanea sativa* Mill.) in Europe. Ecol. Mediterr. 30 (2), 179–193.

Conedera, M., Krebs, P., Tinner, W., Pradella, M., Torriani, D., 2004b. The cultivation of *Castanea sativa* (Mill.) in Europe, from its origin to its diffusion on a continental scale. Veg. Hist. Arcaeobot. 13, 161–179. https://doi.org/10.1007/s00334-004-0038-7.

Cutini, A., 2000. Biomass, litterfall and productivity in chestnut coppices of various age at Monte Amiata (Central Italy). Ecol. Mediterr. 26, 33–41. https://doi.org/10.3406/ecmed.2000.1889.

Díaz-Varela, E., Álvarez-Álvarez, P., Roces-Díaz, J., Rodríguez-Morales, B., 2018. The contribution of chestnut orchard recovery projects for effective area-based conservation: Two cases in Asturias (North-West Spain). In: Sustainable Use of Biodiversity in Socio-Ecological Production Landscapes and Seascapes (SEPLS) and Its Contribution to Effective Area-Based Conservation. Publisher, United Nations University, pp. 26–37.

EUROCASTANEA, 2019. Le livre blanc de la chataigne européene. Avilable online: Livre Blanc (eurocastanea.org).

Fernández-López, J., Alía, R., 2003. Chesnut. *Castanea sativa*. Technical guidelines for genetic conservation and use. EUFORGEN.

Gonzalo, J., 2010. Diagnosis fitoclimática de la España peninsular. Hacia un modelo de clasificación funcional de la vegetación y de los ecosistemas peninsulares españoles. Serie Técnica: Naturaleza y Parques Nacionales. Ministerio de Medio Ambiente y Medio Rural y Marino. Organismo Autónomo Parques Nacionales. ISBN:978-84-8014-787-3.

Griscom, B.W., Adams, J., Ellis, P.W., Houghton, R.A., Lomax, G., Miteva, D.A., Schlesinger, W.H., Shoch, D., Siikamäki, J.V., Smith, P., Woodbury, P., Zganjar, C., Blackman, A., Campari, J., Conant, R.T., Delgado, C., Elias, P., Gopalakrishna, T., Hamsik, M.R., Herrero, M., Kiesecker, J., Landis, E., Laestadius, L., Leavitt, S.M., Minnemeyer, S., Polasky, S., Potapov, P., Putz, F.E., Sanderman, J., Silvius, M.,

Wollenberg, E., Fargione, J., 2017. Natural climate solutions. Proc. Natl. Acad. Sci. U. S. A. 114, 11645–11650. https://doi.org/10.1073/pnas.1710465114.
Huang, S., Price, D., Titus, S.J., 2000. Development of ecoregion-based height - diameter models for white spruce in boreal forests. For. Ecol. Manage. 129, 125–141.
Jacobs, D.F., Selig, M.F., Severeid, L.R., 2009. Aboveground carbon biomass of plantation-grown American chestnut (*Castanea dentata*) in absence of blight. For. Ecol. Manage. 258, 288–294. https://doi.org/10.1016/j.foreco.2009.04.014.
Kaitaniemi, P., 2004. Testing the allometric scaling laws. J. Theor. Biol. 228, 149–153. https://doi.org/10.1016/j.jtbi.2003.12.007.
Krebs, P., Pezzatti, G.B., Beffa, G., Tinner, W., Conedera, M., 2019. Revising the sweet chestnut (*Castanea sativa* Mill.) refugia history of the last glacial period with extended pollen and macrofossil evidence. Quat. Sci. Rev. 206, 111–128. https://doi.org/10.1016/j.quascirev.2019.01.002.
Kurz, W., Beukema, S., Apps, M., 1996. Estimation of root biomass and dynamics for the carbon budget model of the Canadian forest sector. Can. J. For. Res. 26, 1973–1979.
Lara-Gómez, M.A., Navarro-Cerrillo, R.M., Ceacero, C.J., Ruiz-Goméz, F.J., Díaz-Hernández, J.L., Palacios Rodriguez, G., 2020. Use of Aerial Laser Scanning to Assess the Effect on C Sequestration of Oak (*Quercus ilex* L. subsp. ballota [Desf.] Samp-*Q. suber* L.) Afforestation on Agricultural Land. Geosciences 2020, 10, 41.
Ledo, A., Paul, K.I., Burslem, D.F.R.P., Ewel, J.J., Barton, C., Battaglia, M., Brooksbank, K., Carter, J., Eid, T.H., England, J.R., Fitzgerald, A., Jonson, J., Mencuccini, M., Montagu, K.D., Montero, G., Mugasha, W.A., Pinkard, E., Roxburgh, S., Ryan, C.M., Ruiz-Peinado, R., Sochacki, S., Specht, A., Wildy, D., Wirth, C., Zerihun, A., Chave, J., 2018. Tree size and climatic water deficit control root to shoot ratio in individual trees globally. New Phytol 217, 8–11. https://doi.org/10.1111/nph.14863.
Lee, S.J., Yim, J.S., Son, Y.M., Son, Y., Kim, R., 2018. Estimation of forest carbon stocks for national greenhouse gas inventory reporting in South Korea. Forests 9, 1–12. https://doi.org/10.3390/f9100625.
Lemaire J. (ed), 2008. Sylviculture du châtaignier: des outils simples et performants. Forêt-Enterprise 179. 64 p.
Lewis, S.L., Wheeler, C.E., Mitchard, E.T.A., Koch, A., 2019. Restoring natural forests is the best way to remove atmospheric carbon. Nature 568, 25–28. https://doi.org/10.1038/d41586-019-01026-8.
Mäkinen, A., Korpela, I., Tokola, T., Kangas, A., 2006. Effects of imaging conditions on crown diameter measurements from high-resolution aerial images. Can. J. For. Res. 36, 1206–1217. https://doi.org/10.1139/X06-011.
McKay, H.M., Harrison, A.J., Connolly, T., Forster, J., Gregory, S., Smith, E., Clark, J., 2022. Early performance of eight broadleaved species grown as short rotation forest in England. Forestry 98 (1), 13–27. https://doi.org/10.1093/forestry/cpab033.
Menéndez-Miguélez, M., Canga, E., Barrio-Anta, M., Majada, J., Álvarez-Álvarez, P., 2013. A three level system for estimating the biomass of *Castanea sativa* Mill. coppice stands in north-west Spain. For. Ecol. Manage. 291, 417–426. https://doi.org/10.1016/j.foreco.2012.11.040.
Menéndez-Miguélez, M., Álvarez-Álvarez, P., Majada, J., Canga, E., 2015. Effects of soil nutrients and environmental factors on site productivity in *Castanea sativa* Mill. coppice stands in NW Spain. New For. 46, 217–233.
Menéndez-Miguélez, M., Álvarez-Álvarez, P., Majada, J., Canga, E., 2016. Management tools for *Castanea sativa* coppice stands in northwestern Spain. Bosque 37 (1), 119–133.
Menéndez-Miguélez, M., Calama, R., del Río, M., Madrigal, G., López-Senespleda, E., Pardos, M., Ruiz-Peinado, R., 2022. Biomass and bioenergy species-specific and generalized biomass models for estimating carbon stocks of young reforestations. Biomass Bioenergy 161, 106453. https://doi.org/10.1016/j.biombioe.2022.106453.
Menéndez-Miguélez, M., del Río, M., Ruiz-Peinado, R., Pardos, M., López-Senespleda, E., Madrigal, G., Vivanco, P., Calama, R. 2022b. Ecuaciones preliminares de biomasa en repoblaciones jóvenes y estudio de las variables de mayor influencia en su producción y crecimiento. In proceedings 8th Spanish Forest Congress. Lleida 27th June- 1st July 2022.
Mokany, K., Raison, R.J., Prokushkin, A.S., 2006. Critical analysis of root:shoot ratios in terrestrial biomes. Glob. Change Biol. 12, 84–96.
Montero, G., Ruiz-Peinado, R., Muñoz, M., 2005. Producción de biomasa y fijación de CO2 por los bosques españoles. Madrid.
Montero, G., Ortega Muela, C., Cañellas, I., Bachiller, A., 1999. Productividad aérea y dinámica de nutrientes en una repoblación de *Pinus pinaster* Ait. sometida a distintos regímenes de claras. Investig. Agrar. Sist. y Recur. For. 8, 175–206. https://doi.org/10.5424/637.
Palacios-Rodríguez, G., Quinto, L., Lara-Gómez, M.A., Pérez-Romero, J., Recio, J.M., Álvarez-Romero, M., Cachinero-Vivar, A.M., Hernández-Navarro, S., Navarro-Cerrillo, R.M., 2022. Carbon Sequestration in Carob *(Ceratonia siliqu*a L.) Plantations under the EU Afforestation Program in Southern Spain Using Low-Density Aerial Laser Scanning (ALS) Data. Forests 13, 285. https://doi.org/10.3390/f13020285.
Patrício, M.S., Nunes, L., 2017. Density management diagrams for sweet chestnut high-forest stands in Portugal. iForest 10, 865-870. https://doi: 10.3832/ifor2411-010.
Patricio, M.S., Tomé, M., 2018. Allometri equations for predicting mineralomass in high-forest chestnut stands in Portugal. In: Serdar, U., Çelik, H. (Eds.), Proc. VI Intl. Chestnut Congress, Acta Hort. 1220, pp. 125-132.
Patrício, M.S., Tomé, M., Monteiro, M.L., 2005. Biomass Equations for *Castanea sativa* High Forest in the Northwest of Portugal. Acta Horticulturae 693:727-732. https://doi.10.17660/ActaHortic.2005.693.98.
Patrício, M.S., Monteiro, M.L., 2005. Biomass equations for *Castanea sativa* High Forest in the Northwest of Portugal. In: Abreu, .G., Rosa, E., Monteiro, A.A. (Eds.), Proc. Third Intl. Chestnut Congress, Acta Hort. 693, pp. 727-732.
Pereira-Lorenzo, S., Ramos-Cabrer, A.M., 2004. Chestnut an ancient crop with future. In Production Practices and Quality Assessment of Food Crops, Volume 1 Preharvest Practices. Eds Dris, R. and Jain, S.M., pp 105-161.
Pérez-Cruzado, C., Merino, A., Rodríguez-Soalleiro, R., 2011. A management tool for estimating bioenergy production and carbon sequestration in *Eucalyptus globulus* and *Eucalyptus nitens* grown as short rotation woody crops in north-west Spain. Biomass Bioenergy 35, 2839–2851. https://doi.org/10.1016/j.biombioe.2011.03.020.
Pillsbury, N.H., McDonald, P.M., Simon, V., 1995. Reliability of Tanoak Volume Equations When Applied to Different Areas. West. J. Appl. For. 10 (2), 72–78. https://doi.org/10.1093/wjaf/10.2.72.
Porté, A., Trichet, P., Bert, D., Loustau, D., 2002. Allometric relationships for branch and tree woody biomass of Maritime pine (*Pinus pinaster* Ait.). For. Ecol. Manage. 158, 71–83. https://doi.org/10.1016/S0378-1127(00)00673-3.
Prada, M., González-García, M., Majada, J., Martínez-Alonso, C., 2019. Development of a dynamic growth model for sweet chestnut coppice: A case study in Northwest Spain. Ecol. Modell. 409, 108761 https://doi.org/10.1016/j.ecolmodel.2019.108761.
Roces-Díaz, J.V., Jiménez-Alfaro, B., Chytrý, M., Díaz-Varela, E.R., Álvarez-Álvarez, P., 2018a. Glacial refugia and mid-Holocene expansion delineate the current distribution of *Castanea sativa* in Europe. Palaeogeogr. Palaeocl. 491, 152–160. https://doi.org/10.1016/j.palaeo.2017.12.004.
Roces-Díaz, J.V., Díaz-Varela, E.R., Barrio-Anta, M., Álvarez-Álvarez, P., 2018b. Sweet chestnut agroforestry systems in North-western Spain: Classification, spatial distribution and an ecosystem services assessment. For. Syst. 27, 1–14. https://doi.org/10.5424/fs/2018271-11973.
Ruiz-Peinado, R., Montero, G., del Rio, M., 2012. Biomass models to estimate carbon stocks for hardwood tree species. For. Syst. 21, 42–52. https://doi.org/10.5424/fs/2112211-02193.
Salazar, S., Sánchez, L.E., Galindo, P., Santa-Regina, I., 2010. Above-ground tree biomass equations and nutrient pools for a paraclimax chestnut stand and for a climax oak stand in the sierra de Francia mountains, Salamanca. Spain. Sci. Res. Essays 5, 1294–1301.
Sammut, C., Webb, G.I. (Eds.), 2011. Encyclopedia of Machine Learning. Springer, Boston, MA. https://doi.org/10.1007/978-0-387-30164-8_469.
Santa Regina, I., 2000. Organic matter distribution and nutrient fluxes within a sweet chestnut (*Castanea sativa* Mill.) stand of the Sierra de Gata. Spain. Ann. For. Sci. 57, 691–700.
SAS Inc., 2004. SAS/STAT®. 9.1. User's Guide. Cary, NC.
Somogyi, Z., Cienciala, E., Mäkipää, R., Muukkonen, P., Lehtonen, A., Weiss, P., 2007. Indirect methods of large-scale forest biomass estimation. Eur. J. For. Res. 126, 197–207.
Waring, B., Neumann, M., Prentice, I.C., Adams, M., Smith, P., Siegert, M., 2020. Forests and Decarbonization – Roles of Natural and Planted Forests. Front. For. Glob. Chang. 3, 1–6. https://doi.org/10.3389/ffgc.2020.00058.
Xiang, W., Li, L., Ouyang, S., Xiao, W., Zeng, L., Chen, L., Lei, P., Deng, X., Zeng, Y., Fang, J., Forrester, D.I., 2021. Effects of stand age on tree biomass partitioning and allometric equations in Chinese fir (*Cunninghamia lanceolata*) plantations. Eur. J. For. Res. 140, 317–332. https://doi.org/10.1007/s10342-020-01333-0.
Yamaura, Y., Yamada, Y., Matsuura, T., Tamai, K., Taki, H., Sato, T., Hashimoto, S., Murakami, W., Toda, K., Saito, H., Nanko, K., Ito, E., Takayama, N., Tsuzuki, N., Takahashi, M., Yamaki, K., Sano, M., 2021. Modeling impacts of broad-scale plantation forestry on ecosystem services in the past 60 years and for the future. Ecosyst. Serv. 49, 101271 https://doi.org/10.1016/j.ecoser.2021.101271.
Zianis, D., Mencuccini, M., 2004. On simplifying allometric analyses of forest biomass. For. Ecol. Manage. 187, 311–332. https://doi.org/10.1016/j.foreco.2003.07.007.
Zianis, D., Muukkonen, P., Mäkipää, R., Mencuccini, M., 2005. Biomass and stem volume equations for tree species in Europe. Silva Fennica Monographs.